

Dynamic ultrafast laser beam shaping for material processing at the imaging plane using a spatial light modulator

Jiangning Li^{a,*}, Zheng Kuang^a, Juan Godoy Vilar^a, Geoff Dearden^a, Walter Perrie^a,
Stuart Edwardson^a

^aLaser Group, Centre for Materials and Structures, School of Engineering, University of Liverpool, Brownlow Street, Liverpool L69 3GQ, UK

Abstract

We have demonstrated an original precise laser beam shaping technique for ultra-short pulse laser material processing by two-dimension (2D) reflectivity tuning a spatial light modulator (SLM). Intensity masks derived from real beam profiles were generated using Matlab. Interesting shapes such as flat-top, slop, steps and blow with designed intensity distributions were obtained at the diffraction near-field and reconstructed at an image plane of an f-theta lens ($f \sim 100\text{mm}$) for material processing using a picosecond laser source. The size of the shaped beam was approximately $34.5\mu\text{m}$ at the image plane, which was comparable to the beam waist at the focal plane and ensured sufficient fluence for laser material ablation.

© 2016 The Authors. Published by Bayerisches Laserzentrum GmbH

Keywords: ultrafast laser; beam shaping; spatial light modulator; gray level geometric mask; dynamic control

1. Introduction

In recent years, the ultrafast laser has attracted increasing interests as a high precision high quality tool for micro-processing on various materials. Metals (Momma et al., 1996; Vonder Linde & Sokolowski-Tinten, 2000), semiconductors (Sundaram & Mazur, 2002), dielectrics (Sudrie et al., 2001; Schaffer et al., 2004; Osellame et al., 2003) and biological materials (Konig et al., 2002; Watanabe et al., 2004) have been processed by ultrafast laser to generate a very small heat affected zone around the irradiated area. Nowadays, ultrafast laser systems, such as picosecond fibre lasers, have been increasingly employed by manufacturing industries because of the more compact system and lower cost.

One of the characteristics of ultrafast laser material processing is that the shape of the processed area is very close to the input beam's intensity distribution thanks to the well-defined ablation threshold. This has motivated some efforts in the field of ultrafast laser beam shaping. From the use of amplitude mask projection and diffractive optical elements (DOEs) (Momma et al., 1998) to deformable mirrors (Thomson et al., 2008), different techniques have been attempted to shape ultrafast laser beams for various applications. Multiple annular beams were generated at focal plane for ultrafast laser micro-drilling with diffractive axicon phases using a spatial light modulator (SLM) (Kuang et al., 2014). Sanner et al. (2005a, 2007b) successfully obtained top-hat, doughnut, square, and triangle beam shapes at focal plane by programmable wave-front modulations using a non-pixelated optically addressed light valve.

The phase modulation to the incident laser beam can be complicated in order to produce a desired shape at focal plane (i.e. far field). Although algorithms based on time-consuming iterative calculations, such as Gerchberg and Saxton (1972), were attempted to calculate the phase holograms for the far field beam shaping, the accuracy was still not perfect due to the complex nature of light diffraction (Liu & Taghizadeh, 2002; Beck et al., 2011). We recently demonstrated an interesting beam shaping technique using a spatial light modulator (SLM), where arbitrary beam intensity shapes were easily obtained by geometric masks at diffraction near-field and then reconstructed at an imaging plane with a much smaller size comparable to the beam waist at focal plane (Kuang et al., 2015; Li et al., 2016).

* Corresponding author. Tel.: +44-07453443442.
E-mail address: sgjli14@liverpool.ac.uk

In order to further improve the shaping accuracy, we report in this paper intensity masks derived from real beam profiles rather than Gaussian approximations. The masks were generated using Matlab and can be applied on an SLM in real time. Interesting shapes such as flat-top, slope, steps and bowl with designed intensity distributions were obtained at the diffraction near-field and reconstructed at an image plane of an f-theta lens ($f \sim 100\text{mm}$) for material processing using a picosecond laser source. The size of the shaped beam was approximately $34.5\mu\text{m}$ at the image plane, which was comparable to the beam waist at the focal plane and ensured sufficient fluence for laser material ablation.

2. Experimental

A schematic of the experimental setup is shown in Fig.1. A linear polarized laser beam output (Beam diameter: $\text{Dia.} \approx 0.8\text{mm}$, pulse duration: $t_p=20\text{ps}$, wavelength: $\lambda=1064\text{nm}$, and repetition rate: $F=200\text{kHz}$) generated by a picosecond fibre laser system (Fianium) passed through a half wave plate used for adjusting the state of polarization, a beam expander ($M \approx 6$ and expanded beam diameter $\approx 4.8\text{mm}$), two plane mirrors for adjusting the beam path, and illuminated on a reflective, liquid crystal SLM (Holoeye LC-R2500).

A polarization analyzer was placed after the SLM to modulate the shape and intensity distribution of laser beam. The SLM has twisted nematic microdisplay cells. The orientation of the molecules differs by $0-45$ degree between the top and the bottom of the liquid crystal (LC) cell and is arranged in a helix-like structure. The output beam polarization rotates a certain angle depending on how much the relevant LC cell is twisted. Amplitude modulation is hence achieved by adding a polarizer (analyzer) afterward.

When observing the laser beam profile, the beam was reflected by a flip mirror (Fig.1 point I) and then passed through two positive lenses (focal length: $f_0=200\text{mm}$) from a $4f$ system to reach a CCD camera-based laser beam profiler (Thorlabs). When processing the flip mirror was removed from the optical alignment. A long beam path is required to bring the image plane close to the focal plane of the F-theta lens, this will be discussed later. The beam therefore traversed a long distance by multiple reflections on a series of mirrors before reaching a scanning galvanometer, and a focusing F-theta lens ($f_{f,\theta}=100\text{mm}$). Machining samples were mounted on a three-axis motion control stage (Aerotech), placed under the F-theta lens.

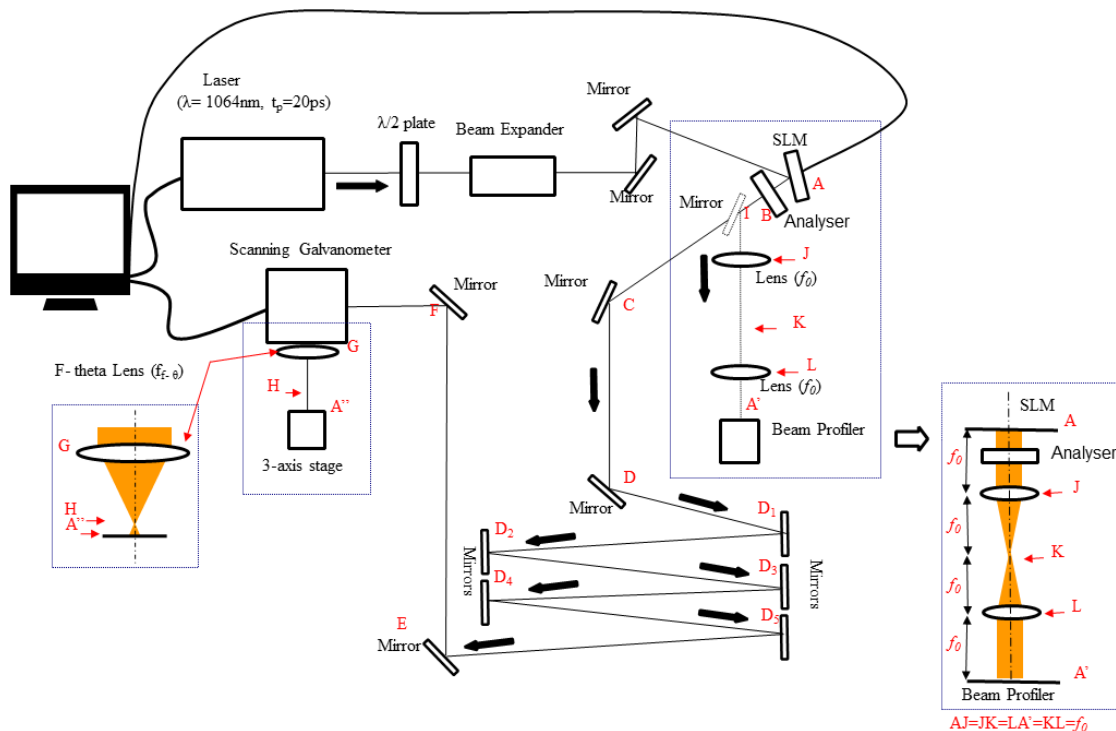


Fig. 1. Experimental setup.

3. Result and Discussions

3.1. Generation of laser beam with designed shape and intensity distribution

Holoeye LC-R 2500 is a reflective Liquid Crystal on Silicon (LCoS) based spatial light modulator (SLM). The structure of the LCoS is 45° twisted nematic (TN) microdisplay cells. When applying an input voltage signal from 0 to maximum (controlled by the displayed mask's grey level from 0 to 255), the orientation of the molecules changes accordingly by 0 - 45° between the top and the bottom of the LC cell, creating a helix-like structure. The output polarization hence varies from 0° to 45° accordingly. By using a geometric grey level gradient mask and an analyzer placed after SLM, an accurate amplitude modification can be achieved.

Fig.2 shows the reflectivity (R) versus the grey level (GL) of the mask. The relationship between R and GL is approximately linear, as shown in figure 2.

$$R = f(GL) = 0.001GL + 0.2006 \quad GL \in [0,255] \quad (1)$$

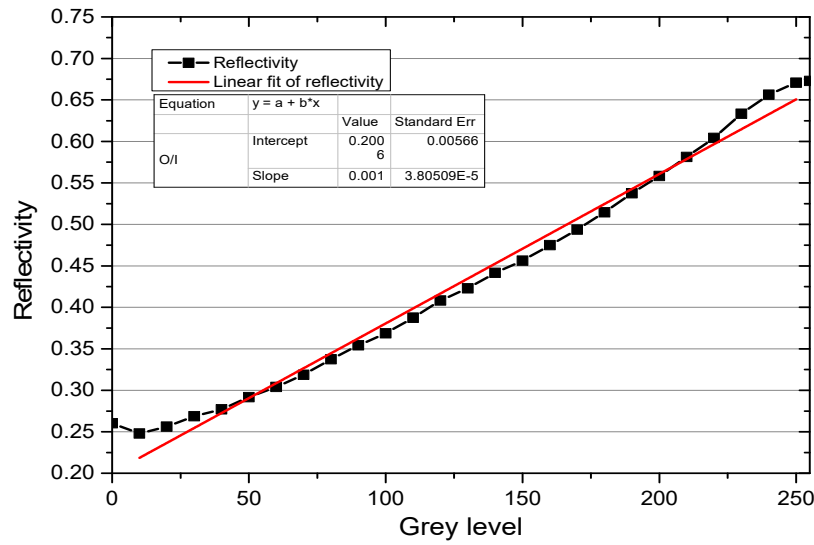


Fig. 2. The SLM reflectivity versus mask grey level.

Fig.3 (a) shows the original 3D laser beam profile taken by CCD camera. Fig.3 (b) shows the beam profile in grey level which is used for data modifying. As shown in Fig.3 (c), image data of a 300×300 pixels (1pixel=0.645μm×0.645μm) square is exported from camera and read by Matlab, in which white colour is set as value 0 and black is set as value 255. The intensity per pixel decreases from highest (white) to 0 (black) linearly. In order to obtain other beam profile, the function of required intensity distribution (Y) should be proportional to the result of reflectivity (R) multiply original intensity distribution (O). Where α is a factor to normalize the intensity distribution (Y) between 0 and 1.

$$Y = \alpha \times R \times O \quad (2)$$

By combining equation (1) with (2), we can derive:

$$[GL] = \left(\frac{[Y]}{\alpha [O]} - 0.2006 \right) / 0.001 \quad (3)$$

Where [GL] is a given point in the 300×300 grey level matrix and the value is displayed on the SLM. Each element in the matrix represents a pixel in the beam profile.

For example, to obtain a flat top distribution beam, the equation should be:

Where c is a constant.

$$[GL] = \left(\frac{c}{\alpha[0]} - 0.2006\right)/0.001 \quad (4)$$

To obtain a Gaussian distribution beam, the equation should be:

$$[GL] = \left(\frac{1}{\sigma\sqrt{2\pi}} e^{-\frac{x^2+y^2}{2\sigma^2}} - 0.2006\right)/0.001 \quad (5)$$

Based on equation (3), intensity mask with various shapes and intensity distributions were created using Matlab. As shown in Fig.4, two grey level masks were made to obtain Gaussian distribution (a) and flat top distribution (b). It can be seen in Fig.3 and Fig.4 that there is some unwanted diffraction effects due to optics contamination, which will be optimized in future work.

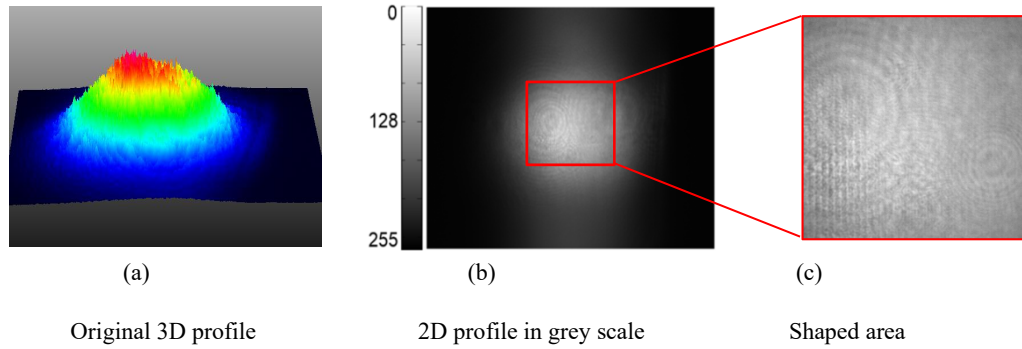


Fig. 3. Original beam profile.

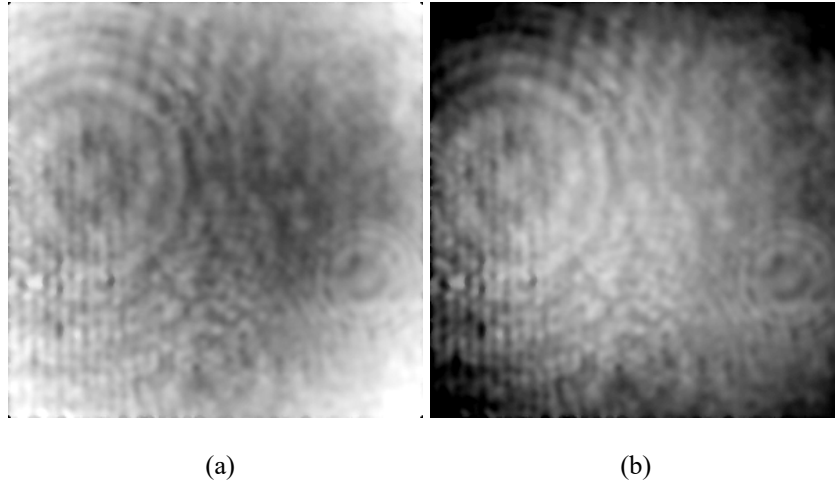


Fig. 4. Grey level gradient masks generated by Matlab.

3.2. Shaping reconstruction at imaging plane of focusing lens

As shown in figure 1, the generated mask shaped the incident beam in near field after SLM at A. The shape was reconstructed after the 4-f optical system at A' for observation using the beam profiler, and also reconstructed at the imaging plane of the F-theta lens, A'', for material processing. As shown in Figure 1, five extra mirrors, D1–D5, were added to significantly increase the distance from the SLM to the focusing F-theta lens, i.e. the object distance. The purpose of this was to reconstruct the shape to a small size comparable to the beam waist. The position of the imaging plane A'' can be calculated, based on the thin lens imaging equation below,

$$\frac{1}{u} + \frac{1}{v} = \frac{1}{f} \quad (6)$$

Where, $u \approx 11000\text{mm}$ is the object distance, i.e. the distance from the SLM(A) to the F-theta lens(G), $f=100\text{mm}$ is the focal length of the F-theta lens and v is the image distance, i.e. the distance from the F-theta lens(G) to image plane (A'').

$$v = \frac{fu}{u-f} \approx 100.9\text{mm} \quad (7)$$

The gap between the focal and imaging plane is:

$$d = v - f \approx 0.9\text{mm} \quad (8)$$

The magnification of the image system is $M \approx 1/110$. The original expanded beam size is approximately 4.8mm. The diameter of reconstructed beam at A'' can be calculated to be approximately 43.6 μm , which was comparable to the beam waist at the focal plane H.

Beam shaping results observed by CCD camera at A'

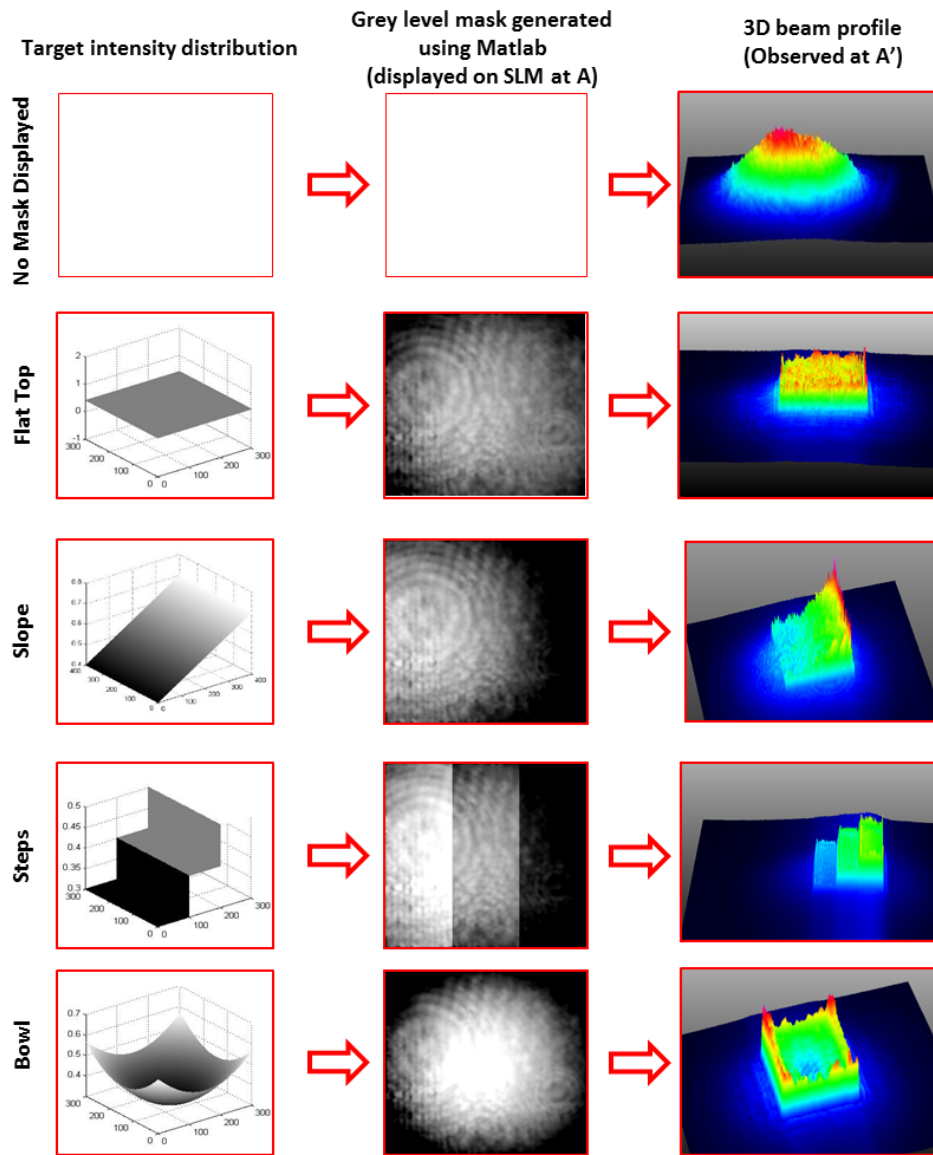


Fig. 5. Grey level masks generated by Matlab and beam profile observed at A'.

As shown in Fig.5, the first column shows the target intensity distribution we want to achieve, the second column shows the grey level mask generated based on original beam profile, while the third column shows the

corresponding beam profiles observed at A'. The original beam profile can be seen to be circular and has a Gaussian distribution. Using the derived grey level masks both the outline profile and inside intensity distribution has been shaped.

4. Conclusions

We have demonstrated an original precise laser beam shaping technique for ultra-short pulse laser material processing by two-dimension (2D) reflectivity tuning a spatial light modulator (SLM). Intensity masks derived from real beam profiles were generated using Matlab. Interesting shapes such as flat-top, slope, steps and bowl with designed intensity distributions were obtained at the diffraction near-field and reconstructed at an image plane of an f-theta lens ($f \sim 100\text{mm}$) for material processing using a picosecond laser source. The size of the shaped beam was approximately $34.5\mu\text{m}$ at the image plane, which was comparable to the beam waist at the focal plane and ensured sufficient fluence for laser material ablation. Future work will confirm the applicability of the technique in material processing.

References

- Beck, R., Parry, J., Shephard, J., & Hand, D. (2011). Adaptive extra cavity beam shaping for application in nanosecond laser micromachining. *Proceeding of SPIE*. doi:10.1117/12.875177.
- Gerchberg, R., & Saxton, W. O. (1972). A practical algorithm for the determination of the phase from image and diffraction plane pictures. *Optik*, 35, 237.
- König, K., Krauss, O., & Riemann, I. (2002). Intratissue surgery with 80-MHz nanosecond femtosecond laser pulses in the near infrared. *Opt Express*(20), 171-6.
- Kuang, Z., Li, J., Edwardson, W., Perrie, W., Liu, D., & Dearden, G. (2015). Ultrafast laser beam shaping for material processing at imaging plane by geometric masks using a spatial light modulator. *Optics and Laser in Engineering*, 70, 1-5.
- Kuang, Z., Perrie, W., Edwardson, S., Fearon, E., & Dearden, G. (2014). Ultrafast laser parallel micro drilling using multiple annular beams generated by a spatial light modulator. *JPhysD:Applphys*, 47, 115501.
- Li, J., Kuang, Z., Edwardson, S., Perrie, W., Liu, D., & Dearden, G. (2016). Imaging-based amplitude laser beam shaping for material processing by 2D reflectivity tuning of a spatial light modulator. *Applied Optics*, 55(5), 1095-1100.
- Liu, J., & Taghizadeh, M. (2002). Iterative algorithm for the design of diffractive phase elements for laser beam shaping. *Opt Lett*, 27, 1463.
- Momma, C., Chichkov, B., Nolte, S., von Alvensleben, F., Tunnermann, A., & Welling, H. (1996). Short pulse laser ablation of solid targets. *Opt Commun*(129), 134-42.
- Momma, C., Nolte, S., Kamlage, G., von Alvensleben, F., & Tunnermann, A. (1998). Beam delivery of femtosecond laser radiation by diffractive optical elements. *Appl Phys A*, 67, 517-20.
- Osellame, R., Taccheo, S., Marangoni, M., Ramponi, R., Laporta, P., & Polli, D. (2003). Femtosecond writing of active optical waveguides with astigmatically shaped beams. *J Opt Soc Am B*(20), 1559-67.
- Sanner, N., Huot, N., Audouard, E., Larat, C., & Huignard, J. (2007). A practical algorithm for the determination of the phase from image and diffraction plane pictures. *Opt Laser Eng*, 45, 737-41.
- Sanner, N., Huot, N., Audouard, E., & Larat, C. (2005). Programmable focal spot shaping of amplified femtosecond laser pulses. *Opt Lett*, 30(12), 1479-81.
- Schaffer, C., Jamison, A., & Mazur, E. (2004). Morphology of femtosecond laser-induced structural changes in bulk transparent materials. *Appl Phys Lett*(84), 1441-3.
- Sudrie, L., Franco, M., Prade, B., & Mysyrowic, A. (2001). Study of damage in fused silica induced by ultra-short IR laser pulses. *Opt Commun*(191), 333-9.
- Sundaram, S., & Mazur, E. (2002). Inducing and probing non-thermal transitions in semiconductors using femtosecond laser pulses. *Nat Mater*(1), 217-24.
- Thomson, R., Bockelt, A., Ramsay, E., Beecher, S., Greenaway, A., & Kar, A. (2008). Shaping ultrafast laser in scribed optical wave guides using a deformable mirror. *Opt Express*, 16(17), 517-20.
- Vonder Linde, D., & Sokolowski-Tinten, K. (2000). The physical mechanisms of short-pulse laser ablation. *Appl Surf Sci*(154-155), 1-10.
- Watanabe, W., Arakawa, N., Matsunaga, S., Higashi, T., Fukui, K., & Isobe, K. (2004). Femtosecond laser disruption of subcellular organelles in a living cell. *Opt Express*(12), 4203-13.